HHS Public Access

Author manuscript

J Mol Recognit. Author manuscript; available in PMC 2017 August 23.

Published in final edited form as:

J Mol Recognit. 2012 July ; 25(7): 393–403. doi:10.1002/jmr.2196.

Protein Interface Remodeling in a Chemically Induced Protein Dimer

Brian R. White, **Jonathan C.T. Carlson**, **Jessie L. Kerns**, and **Carston R. Wagner***

Department of Medicinal Chemistry, College of Pharmacy, University of Minnesota, Minneapolis, MN 55455

Abstract

While the development of chemically induced, self-assembled protein-based materials is rapidly expanding, methods for directing their assembly in solution are sparse, and problems of population heterogeneity remain. By exerting control over the assembly of advanced protein structures, new classes of ordered protein nanomaterials become feasible, affecting numerous applications ranging from therapeutics to nanostructural engineering. Focusing on a protein-based method for modulating the stability of a chemically induced DHFR dimer, we demonstrate the sensitivity of a methotrexate competition assay in determining the change in DHFR-DHFR binding cooperativity via interfacial mutations over a 1.3 kcal/mol range. This represents a change of more than 40% of the dimer complex binding energy conferred from protein-protein cooperativity (~3.1 kcal/mol). With the development of this investigative system and refinement of protein-based techniques for complex stability modulation, the directed assembly of protein nanomaterials into hetero-complexes and a concomitant decrease in population heterogeneity becomes a realizable goal.

Keywords

DHFR; protein interface; chemically induced dimerization; nanostructures; dimerizer; methotrexate; competition; self-assembly

Introduction

Molecular recognition plays a key role in defining the protein and nucleic acid interactions that create and operate living systems. The library of known protein-protein interactions has been extensively studied in an effort to uncover its diverse role in biological processes as well as develop therapeutic tools that can exploit such interactions for the treatment of disease.(Salwinski, Miller et al. 2004; Keskin, Gursoy et al. 2008; Reilly, Cunningham et al. 2009) A great deal of effort has been put forth toward delineating the composition and role of interfacial amino acids,(Glaser, Steinberg et al. 2001; Ofran and Rost 2003) the contribution of thermodynamic forces to protein complex stability,(Hendsch and Tidor 1999; Sheinerman, Norel et al. 2002) and the mechanisms by which two proteins go about recognizing each other in a veritable sea of macromolecules.(Young, Jernigan et al. 1994; Lo

*To whom correspondence should be addressed: C. R. Wagner, University of Minnesota, Dept. of Medicinal Chemistry, 8-174 Weaver-Densford Hall, 308 Harvard St. SE, Minneapolis, MN 55455; Phone: 612-625-2614, wagne003@umn.edu.

Conte, Chothia et al. 1999; Kobe and Kajava 2001) Recent advances in bioinformatics have lead to extensive mining of structural complementarity and sequence similarity data; however, the peculiarities of each protein system have made model generation quite difficult. (Walls and Sternberg 1992; Marcotte, Pellegrini et al. 1999; Uetz, Goit et al. 1999)

Protein interfaces have been well-studied, and it is now understood that the composition of the interface is very similar to the rest of the protein surface.(Jones and Thornton 1996) While charged residues are somewhat less common at interfaces due to the net loss of energy due to desolvation, hydrophobic residues such as Phe, Trp, and Met are prevalent in many cases.(Lo Conte, Chothia et al. 1999; Elcock and McCammon 2001) The sidechain packing at protein interfaces is relatively compact, and this defining characteristic can often be used to differentiate true protein interfaces from crystallographic packing artifacts. (Young, Jernigan et al. 1994; Lo Conte, Chothia et al. 1999) This packing density relates closely to the common incorporation of hydrophobic residues at interfaces as the residue sidechains orient in the densest possible manner to minimize contact with solvent.(Vaskar and Aflalo 1994; Tsai, Lin et al. 1997; Crowley, Otting et al. 2001)

It has been shown that protein complex binding energy is frequently localized in interfacial hotspots, where several key residue interactions contribute the majority of the binding energy.(Clackson and Wells 1995; Bogan and Thorn 1998; Reichmann, Rahat et al. 2007; Geppert, Hoy et al. 2011; Cukuroglu, Gursoy et al. 2012) Extensive effort has been directed toward investigating the nature of these hotspots – notably by methods such as alanine scanning mutagenesis, in which residues are replaced serially with alanine in an effort to quantitate their contributions to overall binding energy.(Bogan and Thorn 1998; Thorn and Bogan 2001; Hall, Grove et al. 2011; Liu, Li et al. 2011) On the theoretical front, computational alanine scanning(Massova and Kollman 1999), free energy decomposition(Gohlke and Case 2004) and molecular dynamics(Chowdhury, Shi et al. 2009)have become effective methods for the determination of individual residue contributions to binding energy, resolved even to net contributions from the backbone and sidechain independently. The realization that binding energies are localized in this manner is an important discovery having the potential to drive research toward the design of tailored protein interfaces wherein practical structural and functional modifications may be achieved.

Complementing theoretical work, bench work by Cunningham and Wells revealed that replacement of key residues at the recognition site of human growth hormone (hGH) with alanine modified its affinity for its biological targets – the hGH and prolactin receptors. (Cunningham and Wells 1991; Lowman, Cunningham et al. 1991) While the wild-type enzyme binds each with equivalent affinity, replacement of the key residues yielded a 34,000-fold selectivity for the hGH receptor. Other investigations have utilized the mass reconfiguration of electrostatic interactions as well as the replacement of buried polar residues with nonpolar isosteres.(Hendsch, Jonsson et al. 1996; Hendsch, Nohaile et al. 2001) Further work assessing the interplay of electrostatic and hydrophobic interactions has also shown the stabilizing and destabilizing effects of these modifications. (Camacho, Ma et al. 2006; Johnson, Horne et al. 2011; Lewis and Kuhlman 2011)

In the context of therapeutics, protein interface remodeling is an attractive pursuit as the selective inhibition of protein complexation represents the ability to control a wide array of biological mechanisms.(Mandell and Kortemme 2009; Karanicolas, Com et al. 2011; Smith and Kortemme 2011) Small molecule inhibition would achieve this goal, in effect reshaping the interface to render it non-complementary.(Arkin and Wells 2004; Sillerud and Larson 2005; Garner and Janda 2011; Meireles and Mustata 2011) However, this has remained an elusive target due to the topologically bland surfaces present at protein interfaces that often preclude selectivity. Protein surfaces simply lack the key features amenable to rational design that are found in enzyme binding pockets, such as residues that sterically or electrostatically favor the binding of a small molecule.(Cochran 2000) As such, it remains difficult to control protein association at surfaces with small molecule-based techniques.

With the advent of chemically induced dimerization, it has become possible to control the formation of a protein complex. Since the landmark work of Schrieber et al.(Spencer, Wandless et al. 1993), a number of dimerization systems have been well-studied, resulting in a platform technology or toolkit that serves many technical and investigative applications. Examples of these applications include the selective activation of signal transduction pathways,(Spencer, Wandless et al. 1993; Farrar, Alberola-Ila et al. 1996; Luo, Tzivion et al. 1996; Cheng, Yu et al. 2005) localized control over transcription,(Nyanguile, Uesugi et al. 1997; Biggar and Crabtree 2000; Biggar and Crabtree 2001; Rowe, Casey et al. 2007) posttranslational control over protein structure and function,(Mootz and Muir 2002; Mootz, Blum et al. 2003; Xu and Evans 2005; Schwartz, Saez et al. 2007; Stankunas and Crabtree 2007) protein-ligand proximity sensing,(George, Pick et al. 2004; Keppler, Kindermann et al. 2004; Lemercier, Gendreizig et al. 2007) and yeast three-hybrid based bioscreening.(Licitra and Liu 1996; Kley 2004) Much like their investigative counterparts, therapeutic CID systems exert switchable control over signal transduction and gene expression and can also physically inhibit protein-protein interactions that are known to cause disease, such as amyloid plaque formation in Alzheimer's disease.(Neff and Blau 2001; Whitney, Otto et al. 2001; Gestwicki, Crabtree et al. 2004; Carlotti, Zaldumbide et al. 2005; Zhao, Zhao et al. 2005; Kitov, Lipinski et al. 2008) Lastly, chemically induced protein complexation has become a major player in the development of protein-based nanostructures ranging from biotin-linked streptavidin nanoarrays to more elegant tubular and ring-based structures, some of which even retain catalytic activity.(Ringler and Schulz 2003; Carlson, Jena et al. 2006; Ballister, Lai et al. 2008; Chou, So et al. 2008) A comprehensive review of the myriad studies and applications of chemically induced dimerization systems has been previously published,(Fegan, White et al. 2010) but a common theme is the fusion of proteins of interest to a CID "core", effectively creating a proximity switch for the proteins of interest. Given the broad applications of chemically induced dimerization, it becomes easy to see the importance of fine control over the assembly of this core protein complex.

Of the CID systems available, we have focused our investigations on the chemically induced dihydrofolate reductase (DHFR) dimer, first described by Hu and coworkers.(Kopytek, Standaert et al. 2000) The DHFR dimer is selectively assembled via the addition of a bivalent inhibitor of DHFR – bis-MTX-C9 (Figure 1).(Carlson, Kanter et al. 2003) Our characterization of this system has uncovered several key aspects that highlight its suitability for investigating the effects of interfacial point mutations on DHFR dimer stability.(Carlson,

Kanter et al. 2003) First, dimerization only occurs in the presence of a specific ligand; second, the complex can only be disassembled via the addition of a competitive inhibitor of the dimerizer; third, the thermodynamics of complex assembly have been well-characterized. These factors combine to yield a system well-suited to the study of the weak intermolecular interactions that dominate transient protein complexation.(Tang, Iwahara et al. 2006; Morell, Espargaro et al. 2007) Additionally, the relatively small surface area of the DHFR dimer interface (520 $Å^2$) is beneficial since few mutations are necessary to yield relevant data concerning modified dimer behavior.

A number of studies have emerged where assembling proteins into advanced materials is achieved through chemically induced dimerization.(Dotan, Arad et al. 1999; Padilla, Colovos et al. 2001; Ringler and Schulz 2003; Rele, Song et al. 2007; Ballister, Lai et al. 2008) A key aspect of utilizing chemically induced dimerization for protein nanostructural assembly is control over the composition and assembly of the structure. The simplest nanostructure can be envisioned as a complex between two proteins – A and B. Based on statistical analysis, if there is no selectivity for homo- or heterodimer formation, the three species will distribute into a 1:2:1 ratio of AA:AB:BB. Modification of the energetics of any of these three species will perturb this distribution. Ideal selectivity arises from a heterodimer that is substantially lower in energy than either homodimer. Analysis of the dimerization energetics, however, reveals that heterodimerization can be significantly favored if just one of the homodimers can be destabilized. This scenario exists naturally for the Jun-Fos transcription factor pair,(O'Shea, Rutkowski et al. 1989; O'Shea, Rutkowski et al. 1992) and has been demonstrated previously in the engineered version of the Arc repressor designed by Tidor and Sauer.(Hendsch, Nohaile et al. 2001) This somewhat counterintuitive principle is illustrated in Figure 2, and represents an avenue of control over protein assembly if the destabilization of homodimers can be accurately characterized.

In our laboratory, we have previously analyzed the importance of ligand conformational equilibria in the context of chemically induced protein dimerization(Carlson, Kanter et al. 2003) and developed the chemically induced DHFR dimer into a homodimeric $DHFR_2$ fusion protein-based nanoring.(Carlson, Jena et al. 2006; Ballister, Lai et al. 2008; Chou, So et al. 2008) The purpose of the current work is to characterize the role of inter-residue cooperativity present in the DHFR dimer interface. Such interactions are exploited in an effort to perturb the stability of the homodimer with the intent to utilize destabilized homodimeric pairings as a basis for heterodimer selectivity and control over the core complex of chemically induced dimerization systems. This *protein*-directed method differs from present approaches, which rely primarily on *ligand*-directed methods of achieving heterodimerization (i.e. rapamycin, which intrinsically targets two different proteins).(Belshaw, Ho et al. 1996; Choi, Chen et al. 1996; Liberles, Diver et al. 1997) We believe the protein-directed method represents a conceptually attractive and novel technique for achieving an improved level of control over protein recognition and induced dimerization.

Materials and Methods

General

Kits for site-directed mutagenesis and plasmid DNA preparation were obtained from Stratagene and Invitrogen, respectively. Oligonucleotides used as primers in the mutagenesis reaction were obtained from Integrated DNA Technologies through the University of Minnesota BioMedical Genomics Center. Methotrexate, NADPH, and MTX-agarose were purchased from Sigma-Aldrich. Anion exchange chromatography was performed using DE52 DEAE cellulose purchased from Whatman. Competent JM-109 *E. coli* cells were purchased from Promega (Madison, WI). Salts for buffer preparation were of reagent grade and purchased from Mallinckrodt, Fisher, or Sigma-Aldrich. C9-bis-methotrexate (C9-bis-MTX) was synthesized as previously described and purified to ≥99% purity.(Carlson, Kanter et al. 2003) DHF was prepared fresh as previously described and stored under argon at −80°C.(Blakley 1960) All other reagents were of reagent grade or better and purchased from Sigma-Aldrich.

Protein Expression, Purification, and Characterization

To generate mutant ecDHFR plasmids, the Quickchange kit from Strategene was utilized. In short, complementary primer oligonucleotides bearing the mutations of interest were bound to the parent plasmid and PCR cycling achieved exponential generation of the mutated plasmid. Mutated plasmid DNA was recovered from transformed XL1-Blue *E. coli* via the PureLink HiPure Plasmid Miniprep Kit from Invitrogen. Sequencing of the mutated plasmid by the University of Minnesota Microchemical Facility verified the presence of the mutation. Constructs were generated from the pTZwt1-3 plasmid, a gift from the lab of Virginia F. Smith, Pennsylvania State University, Department of Chemistry. Oligonucleotides (reverse primer sequence is complementary to forward) used to introduce the mutations are listed below:

A19H; 5′-C GTT ATC GGC ATG GAA AAC CAC ATG CCA TGG-3′

A19F; 5′-C GTT ATC GGC ATG GAA AAC TTC ATG CCA TGG-3′

A19Y; 5′-C GTT ATC GGC ATG GAA AAC TAC ATG CCA TGG-3′

A19S; 5′-C GTT ATC GGC ATG GAA AAC TCC ATG CCA TGG-3′

A19L; 5′-C GTT ATC GGC ATG GAA AAC CTC ATG CCA TGG-3′

A19Q; 5′-C GTT ATC GGC ATG GAA AAC CAG ATG CCA TGG-3′

A19K; 5′-CGC GTT ATC GGC ATG GAA AAC AAG ATG CCA TGG-3′

A19E; 5′-C GTT ATC GGC ATG GAA AAC GAG ATG CCA TGG-3′

N23F; 5′-G CCA TGG TTC CTG CCT GCA GAT CTC GCC TGG-3′

N23Y; 5′-G CCA TGG TAC CTG CCT GCA GAT CTC GCC TGG-3′

N23S; 5′-G CCA TGG AGC CTG CCT GCA GAT CTC GCC TGG-3′

N23L; 5′-G CCA TGG CTC CTG CCT GCA GAT CTC GCC TGG-3′

N23Q; 5′-G CCA TGG CAG CTG CCT GCA GAT CTC GCC TGG-3′

N23H; 5′-G CCA TGG CAC CTG CCT GCA GAT CTC GCC TGG-3′

N23K; 5′-G CCA TGG AAG CTG CCT GCA GAT CTC GCC TGG-3′

N23E; 5′-G CCA TGG GAG CTG CCT GCA GAT CTC GCC TGG-3′

Mutant plasmid DNA was transformed into the JM109 *E. coli* expression line. Resulting colonies were inoculated into 4 mL LB broth containing 100 μg/mL ampicillin and grown at 37°C overnight with shaking at 250 rpm. Glycerol was added to cell cultures to a final concentration of 15% (v/v) and stocks were frozen at −80°C until use.

For protein expression, starter cultures were prepared using 4 mL LB broth containing 100 μg/mL ampicillin, 20 μg/mL trimethoprim, and a 40 μL inoculation of JM-109 cells bearing the plasmid of interest. These cultures were grown for a minimum of 8 hours at 37°C with shaking at 250 rpm before a 500 μL aliquot was transferred to 50 mL LB containing the same antibiotics and grown for a minimum of 8 hours under the same conditions. 1 L LB broth containing 100 μg/mL ampicillin was inoculated with 10 mL of the 50 mL culture and grown for a minimum of 12 hours under the same growth conditions. The cell OD600 typically reaches >1.3 during this period.

Cells were recovered via centrifugation at 7500g for 15 minutes, then the cells were lysed via a 30 min incubation in lysis buffer (10 mM KH_2PO_4, 100 μM EDTA, 1 mM DTT, 1 mg/mL Lysozyme, pH 8.0) containing 1 Complete© protease inhibitor tablet (Roche) and 8 × 15 seconds sonication. The crude lysate was centrifuged at 40,000g for 40 min at 4°C and the soluble fraction subjected to the addition of 30% (w/v) $(NH_4)_2SO_4$ over 30 min at 4°C with vigorous stirring. Soluble protein was recovered via centrifugation at 40,000g for 20 min at 4°C. The lysate was dialyzed against 4 L equilibration buffer (10 mM KH_2PO_4, 0.1 mM EDTA, 0.5 M KCl, 0.5 mM DTT, pH 6.0) for a minimum of 4 hours at 4°C, then loaded onto a methotrexate agarose column. The bound protein was washed with a high salt buffer (50 mM KH_2PO_4, 1 mM EDTA, 1 M KCl, 1 mM DTT, pH 6.0) until the A280 and A260 of the eluate is ≤0.1, at which time the protein was eluted with folate elution buffer (50 mM KH_2PO_4, 1 mM EDTA, 1 M KCl, 3 mM folic acid, 1 mM DTT, pH 9.0).

Fractions containing DHFR activity as assayed by the DHFR activity assay (see next section) were pooled and dialyzed against 4 × 4 L of Tris dialysis buffer (50 mM Tris, 1 M NaCl, 1 mM EDTA, 0.5 mM DTT, pH 7.2) for a minimum of 4 hours at 4°C each. A final dialysis against 4 L of DEAE equilibration buffer (10 mM Tris, 1 mM EDTA, 1 mM DTT, pH 7.2) for a minimum of 4 hours at 4°C prepared the protein for loading onto a DEAE anion exchange column. The protein was eluted with a gradient of 0 – 40% buffer B over 300 minutes, then 40 – 100% buffer B over the next 420 minutes. Buffer A is the equilibration buffer described above, and buffer B is DEAE elution buffer (10 mM Tris, 1 mM EDTA, 0.5 M KCl, 1 mM DTT, pH 7.2). Collected fractions were measured for A280, A260, and DHFR activity. Purified DHFR was concentrated to ~1 mg/mL via Amicon centrifugal ultrafiltration devices and stored at 4°C until use. Typical protein yield was 5–15 mg per liter of LB culture. The purity of the proteins was assayed by gel filtration and SDS-

PAGE electrophoresis and the mass of the wild-type and mutant proteins verified via LC-MS.

DHFR Activity Assay

All steps, except absorbance measurements, were performed at 4°C. MTEN buffer (50 mM MES, 25 nM Tris, 0.1 M NaCl, 25 mM Ethanolamine, pH 7.0), NADPH stock solution to a final concentration of 100 μM, and an enzyme sample were mixed to a final volume of 1 mL minus the necessary volume of DHF addition. After a 2 minute incubation, a baseline reading at 340 nm was taken to verify zero activity. DHF was then added from a concentrated master stock to a final concentration of 50 μM, the sample was mixed, and the absorbance read at 340 nm for 1 minute. The rate of absorbance decline corresponds to V_o in μM/min and was calculated with the known extinction coefficient for the DHFR catalyzed reaction, 11,300 $M^{-1}cm^{-1}$.(Taira and Benkovic 1988) DHF and NADPH master stock concentrations were estimated spectrophotometrically using the reagents' extinction coefficients at 280 and 340 nm, respectively.

Mutant DHFR K_d Assay

To assay the affinity for MTX to mutant DHFR, a fluorescence assay measuring the quenching of DHFR fluorescence upon MTX binding was employed. DHFR was diluted to a final concentration of 50 nM in 4 mL MTEN buffer and a baseline fluorescence reading taken, scanning emission from 300–400 nm with excitation at 290nm. Serial additions of MTX were performed, and the emission at 340 nm recorded. Data were fit using JMP-IN 4.0 (SAS Institute).

Protein Gel Filtration

Gel filtration samples were prepared as a 5 μM final DHFR concentration in P500 buffer (0.5M NaCl, 50 mM KH_2PO_4, 1 mM EDTA, pH7.0) with 5% (v/v) glycerol. The samples were loaded on to a Sephadex G-75 column (GE Biosciences) on a Beckman System Gold HPLC and eluted at 0.5 mL/min with P500 buffer. The relative peak intensities were quantitated by absorbance at 280 nm.

Protein Concentration Assays

Three methods were employed to obtain accurate protein concentration. First, the Bradford assay was used to estimate the concentration of the protein sample. Second, the A280 of diluted DHFR samples was measured and the extinction coefficient reported by Taira, et al. was used to calculate protein concentration.(Taira and Benkovic 1988) While this extinction coefficient (31,000 $M^{-1}cm^{-1}$) may not accurately represent that of mutant proteins with Tyr mutations, it was found that this error did not introduce significant uncertainty into the concentration estimate. Since the purified DHFR samples contained additional small molecules absorbing at 280 nm, gel filtration of the sample yielded a correction for the optical purity (percentage of the total A280 area under the curve). This correction factor was applied to the A280 concentration estimate. Lastly, DHFR activity was titrated with a known concentration of MTX. The MTX concentration was determined spectrophotometrically

using the extinction coefficient at 302 nm (22,100 $M^{-1}cm^{-1}$) in 0.1 N NaOH.(Seeger, Cosulich et al. 1949)

Competition Experiments

The concentrations of both monovalent and bivalent MTX were assayed spectrophotometrically. The extinction coefficient for bis-MTX was estimated at 47,400 $M^{-1}cm^{-1}$, based on the value reported by Rosowsky and coworkers for a MTX γ-amide. (Rosowsky, Forsch et al. 1984) Stock samples of DHFR:bis-MTX were mixed at a stoichiometry of 2:1.05 and incubated in P500buffer containing 5% glycerol (v/v) for a minimum of 3 hours. The five percent excess of dimerizer was added in order to ensure complete initial dimerization, and was shown to perturb the data far less than other sources of experimental error (data not shown). Complete dimerization of this initial stock was verified by gel filtration chromatography as described. The stock sample was then split and a range of MTX equivalents added (0.5 to 2.5×). Samples were incubated at room temperature for a minimum of 3 hours and assayed via gel filtration. The fraction of dimer present was obtained from corrected integration of the absorbance of the trace at 280 nm. The denaturation curve was then fit as described in the next section to yield the K_{eq}/K_c ratio with Mathematica (Wolfram Research) and Microsoft Excel.

Data Fitting and Error Analysis

Throughout the development of the competition assay, it has become apparent that there are four main contributors to error introduced in the estimation of K_{eq}/K_c – sample preparation, chromatographic separation, peak area integration, and model data fitting. Of these sources, the first and the last are the most significant. While careful sample preparation yields reproducible results, any human error (i.e. the miscalculation of MTX added) has the potential to introduce large errors in the final ratio estimate due to the sensitivity of the dimer to small changes in MTX concentration. Repeated gel filtration and peak integration of a single sample yields variations of less than 2 percent. Due to the complexity of the cubic equation necessary to fit the equilibrium data, the final source of error necessitates an unusual fitting procedure. Since we were unable to derive an analytic solution for Equation 1 (see Results & Discussion), Mathematica (Wolfram Research) was used to generate a series of model data based on various K_{eq}/K_c ratios that were 0.25 apart (i.e. 0.5, 0.75, 1.0, 1.25, 1.5, etc.). This model data was used to construct a reference table of possible denaturation curves, and the solver module in Microsoft Excel was used to fit the experimental data by selecting the value for K_{eq}/K_c that yielded the lowest sum of squared errors (SSE) when compared to a select model data curve. This process was manually repeated using different model curves until the overall lowest SSE value was found, and the corresponding K_{eq}/K_c ratio was taken as the observed value. This data fitting procedure was performed on each of three separate experiments to yield an average observed K_{eq}/K_c ratio as well as the standard deviation.

Results and Discussion

Mutation Scheme Selection and K_d Analysis

Examination of the *E. coli* DHFR (ecDHFR) crystal structure (PDB ID: 4DFR) reveals several candidates for interfacial mutations where residue sidechains interact across the C_2-symmetric interface. The set of interactions that characterize the dimer interface are summarized in Table 1. Inter-backbone interactions that make up a large part of the interface are not ready targets for mutagenesis. Three pairwise interactions, characterized by primarily sidechain interactions, are presented in Figure 3. Of these three, the Ala19 – Asn23 pair is an attractive target for initial experiments due to the close proximity of their sidechains (3–4 Å), their central location in the dimer interface, and the lack of hydrogen bonding present in the pair. Other targets in Table 1 remain viable for future experiments. These design considerations lead us to hypothesize that mutations utilizing Tyr, Ser, Gln, His, Leu, and Phe would allow for the role of steric, hydrophobic, and electrostatic interactions in the thermodynamic stability of the dimer to be defined.

The residues selected for mutation reside in a loop in DHFR known as the M20 loop, named for the central methionine. This particular loop is significant as it plays a central role in ecDHFR catalysis.(Sawaya and Kraut 1997) Previous work evaluating the catalytic mechanism of ecDHFR has demonstrated the ability of the enzyme to tolerate substitutions of these two residues without compromising its catalytic activity.(Nakamura and Iwakura 1999) This evidence further supported our design plans; however, we decided to verify these findings independently.

To more carefully ascertain the effects of mutations in the M20 loop of DHFR, we performed an analysis of the binding affinity for DHFR to MTX via a fluorescence quenching assay (see Methods section). The relatively tight binding constant for DHFR (590 pM)(Appleman, Howell et al. 1988) leads to a high degree of uncertainty in the estimate of K_d due to the narrow window of concentrations leading to a well-fitted binding curve. However, for all mutants except N23F, the K_d remains statistically unaltered (Table 2). In the case of N23F, the binding affinity shows an apparent 4-fold decrease, to approximately 2.9 nM. Reasons for this change in binding affinity may be attributed to long-range inter-residue interactions affecting the MTX binding pocket, decreased mobility of the M20 loop, interaction of the hydrophobic residue with the pteridine ring of MTX, or a combination of all three. While this perturbation in binding affinity may confound competition assay results at lower concentrations, the relatively high concentration of enzyme at which the assay is performed renders this small change irrelevant in the context of our experiment.

Competition Experiments

In order to quantitate the degree to which point mutations stabilize or destabilize the chemically induced DHFR dimer (DHFR CID), we have developed a competition assay wherein a pre-equilibrated DHFR CID is denatured with increasing equivalents of MTX, leading to a curve which can be fit to the following equation:

$$[E_2D]=\frac{K_cK_{a1}K_{a2}(0.5-[E_2D])(1-2[E_2D])^2}{K_{eq}K_{aMTX}{}^2(M_t-E_t+2[E_2D])^2} \quad (1)$$

In this equation, K_{a1} and K_{a2} are the binding affinities for the first and second bis-MTX binding events, and are assumed to be equal to K_{aMTX}, the DHFR-MTX association constant. K_c and K_{eq} are the cooperativity and dimerizer equilibrium constants, respectively; M_t is the total added MTX concentration; E_t is the total enzyme concentration; and $[E_2D]$ represents the experimentally observed dimer concentration in terms of fraction dimer. The relative stability of the mutant dimer complexes represent a modification of the value of K_c, since the K_{eq} for the dimerizer remains constant over the course of the analysis. Therefore, comparison of the K_{eq}/K_c ratio found for each mutant to the wild-type dimer represents the relative effects of point mutations at the interface on cooperativity. These effects can be quantified in terms of energy by utilizing the equation:

$$\Delta\Delta G=-RTln\left(\frac{K_{eq}/K_{c,mut}}{K_{eq}/K_{c,wt}}\right) \quad (2)$$

A typical competition curve, including model denaturation curves based on several K_{eq}/K_c ratios appears in Figure 4. It is apparent that the lower the value of K_c (and hence the larger the value of the ratio), the less stable the induced dimer, and the easier it is to denature the complex.

Interfacial Mutations Modulate Dimer Stability

The results of competition experiments probing the effects of point mutations on the cooperativity in the DHFR CID are summarized in Figure 5. Ratios of the mutant:WT K_{eq}/K_c values and the associated energy perturbations are shown in Table 3 and Figure 6. Globally, the data spans a dynamic range of cooperativity from 0.31 – 2.44 fold destabilization. These data reveal several trends. First, all mutations of Ala19 are destabilizing in nature, the least being A19Y, with a mutant:WT ratio of 1.32. Examination of the DHFR crystal structure, which is isomorphous to the dimerized DHFR crystal structure (obtained from Dr. Vivian Cody, University at Buffalo, Hauptman Woodward Institute, not yet deposited in the protein data bank) shows that the conformations of Ala19 and Asn23 are oriented such that Ala19 is buried within the protein interface, and, as such, is likely less tolerant of modification (Figure 1). In fact, it is the introduction of charge-charge repulsion that affects dimerization more severely than steric bulk (A19E with a ratio of 2.26), likely due to the forced close proximity of the negative charges between Ala19 and Asp144 and the inability of Ala19 to shift to a more stable conformation. The A19H mutation also has a pronounced effect, possibly due to the polar character of this mutation, leading to an increased desolvation penalty associated with the formation of the interface.

Perturbation of Asn23 yields similar results in terms of charge-charge repulsion (see N23E and N23K); however, most mutations at this position are relatively stabilizing. Examination

of the crystal structure indicates that Asn23 is more spatially accommodating than Ala19, as it is capable of reorganizing into the solvent-occupied area surrounding the MTX binding pocket. The implications of this are twofold and are supported by the data. First, the reorientation of charged residues (i.e. Lys23 or Glu23) back into the interior of the interface to escape the desolvation penalty associated with the presence of ionic residues in a solvent-accessible area results in charge-charge repulsion and destabilized pairs. Second, the introduction of hydrophobic residues helps to stabilize the interface as hydrophobic interactions close to solvent can assist in restricting the conformational freedom of the interface, reinforcing interactions in the local area. (Vaskar and Aflalo 1994; Tsai, Lin et al. 1997; Crowley, Otting et al. 2001)

In both cases, the histidine mutation raises interesting questions. Given the pKa of the imidazole of histidine is 6.0, the charge state of this residue will be highly dependent on the environment, and could serve as either a hydrogen bond acceptor in the unprotonated state or a charge center if protonated. At pH 7.0, (91% deprotonated) our experiments indicate that the level of destabilization associated with the His mutation (about 1.8-fold), is not as severe as the destabilization associated with other ionic mutations, but not as stabilizing when compared with other hydrophobic residues. Competition experiments at pH 6.0 show a very high level of destabilization ($\Delta\Delta G$ = 0.85 kcal/mol, data not shown) when a greater percentage (50% vs 9%) of the His sidechain is more likely to be protonated, indicating that charge repulsion is not the only factor responsible for the observed destabilization of the interface at pH 7.0.

While the effects of charge repulsion at the interface are pronounced, the effects of steric bulk and hydrophobicity are subtle and require in-depth examination. To correlate the general trends associated with steric bulk with change in cooperativity, we assessed total residue 19/23 sidechain volume using the data tables from Tsai, et al.(Tsai, Taylor et al. 1999) Surprisingly, in terms of steric bulk, no correlation exists between sidechain volume and $\Delta\Delta G$ (Figure 7). While it is apparent from the crystal structure that mutations at Asn23 have the ability to move relatively freely and are likely insensitive to sidechain bulk, this is particularly surprising for Ala19, given its location deep within the interface. This indicates that although Ala19 may be accommodating enough to permit mutations with increased steric bulk (typical of protein surfaces), ion pairing interactions do not allow for enough spatial freedom on the part of Ala19 to allow for reorganization into a novel, stable conformation. From this, it can be expected that further attempts to destabilize the interface through point mutations should rely primarily on ionic pairing or dipole-dipole interactions.

For exploring correlation between mean 19/23 sidechain hydrophobicity and K_{eq}/K_c, we referenced the quantitative measure of hydrophobicity given by Carugo, et al.(Carugo 2003) A perhaps unsurprising weakly negative (stabilizing) correlation is present in this comparison (Figure 8). Many protein interfaces show a high hydrophobic character, with some of the most highly conserved residues at protein interfaces being Trp, Phe, and Met. (Elcock and McCammon 2001) The low desolvation penalty for a hydrophobic patch on the surface of the protein combined with the tendency to segregate and stabilize away from solvent support the stabilizing effect of introducing hydrophobic residues into the DHFR

interface. In contrast, introducing highly charged or polar residues will achieve interface destabilization and serve to decrease K_c.

Conclusions

The series of mutations we have engineered at the DHFR interface have demonstrated an ability to modulate homodimer stability over a range of at least 1.3 kcal/mol or nearly an order of magnitude change in the cooperativity equilibrium constant. Although this modulation falls short of the energy differences obtained for the hGH receptor (6.1 kcal/mol),(Cunningham and Wells 1991) when considered relative to the comparatively small scale of DHFR-DHFR interface cooperativity, estimated at $\Delta G \leq -3.1$ kcal/mol, this represents a significant change of ~40%.(Carlson, Kanter et al. 2003)

In the course of our study, we have characterized the effects of representative amino acid point mutations at the DHFR dimer interface. The correlation between sidechain hydrophobicity and increased stability reinforces previous findings that hydrophobic hotspots tend to be conserved among protein interfaces, likely due to a lessened desolvation penalty and a gain in enthalpy associated with tighter binding. However, this affinity is likely to be bounded to an extent by the entropic penalties associated with an increase in the rigidity of the interface.(Brooijmans, Sharp et al. 2002) In contrast, destabilization of the interface can be best achieved by introducing electrostatic repulsion. Interestingly, given the relatively tight packing of the DHFR-DHFR interface, the introduction of steric bulk seems to be overshadowed by hydrophobic and electrostatic effects, and can be dismissed as an effective means of DHFR-DHFR interface modulation.

In terms of the development of an investigative tool, we have demonstrated the utility of the competition assay for testing the effects of point mutations on DHFR dimer cooperativity. Whereas other methods for investigating protein interactions such as phage display(Smith 1985) and surface plasmon resonance (SPR) exist that could, in principle, be used for such studies, previous work in our laboratory has indicated problems with both methods. DHFR does not express well as a functional protein on the surface of phage, and while DHFR may be immobilized on a SPR chip and bis-MTX-C9 bound to the protein, the ligand dissociates and washes off the chip before the second DHFR binding event (data not shown). The competition assay represents a highly sensitive method of quantitating mutation effects, especially if the desired outcome is a highly stable interface and increased values for K_c. If characterization of a highly destabilized interface is required, although sensitivity is only moderately decreased in the current model, employing a tighter-binding dimerizer (i.e. trimethoprim-based) would notably increase precision. Due to the favorable energetics associated with chemically induced dimer formation, even in the absence of protein cooperativity, our approach represents an advantage insomuch as highly destabilizing interactions can still be quantitated. In other native dimer systems, excessive destabilization can yield a completely disrupted complex, precluding high-resolution study of the interface.

Given the range technologies in which chemically induced dimerization can be utilized (as discussed in the Introduction), it is apparent that improved control over the “core” dimer pair (i.e. DHFR-DHFR) can lead to improved control over the application of interest. The

selective dimerization of a DHFR fused to “protein A” and a DHFR fused to “protein B” will lead to the induced proximity of protein A to B. Thus, the preparation of heterodimeric pairs would facilitate the design of “co-polymeric” protein polymers and nanostructures. For example, the one could envisage the preparation of self-assembling bispecific antibody nanorings.(Li, Hapka et al. 2008; Li, So et al. 2010) This is but one use in a broad spectrum of applications which could be affected via control over the CID core.

For the DHFR dimer, we have found that the A19E and N23K homodimers are >2-fold destabilized relative to the wild-type homodimer. In the context of the dimer energy landscape, destabilization of either homodimeric species results in a net increase in homodimer free energy and relative stabilization of a heterodimer.(O’Shea, Rutkowski et al. 1989; O’Shea, Rutkowski et al. 1992; Hendsch, Nohaile et al. 2001) As previously mentioned, while current literature methods rely on primarily ligand-directed methods of effecting heterodimerization,(Belshaw, Ho et al. 1996; Choi, Chen et al. 1996; Liberles, Diver et al. 1997) our protein interface design directed method of dimer stability modulation represents an alternative avenue for increased control over protein interactions.

Acknowledgments

BRW was supported by a Chemistry and Biology NIH traineeship (T32 GM008700). This work was supported in part by the NIH (CA120116, CA125360).

References

Appleman JR, Howell EE, et al. Role of aspartate 27 in the binding of methotrexate to dihydrofolate reductase from Escherichia coli. J Biol Chem. 1988; 263(19):9187–9198. [PubMed: 3288632]

Arkin MR, Wells JA. Small-molecule inhibitors of protein-protein interactions: progressing towards the dream. Nat Rev Drug Discovery. 2004; 3(4):301–317. [PubMed: 15060526]

Ballister ER, Lai AH, et al. In Vitro Self-Assembly of Tailorable Nanotubes from a Simple Protein Building Block. Proc Natl Acad Sci USA. 2008; 105:3733. [PubMed: 18310321]

Belshaw PJ, Ho SN, et al. Controlling protein association and subcellular localization with a synthetic ligand that induces heterodimerization of proteins. Proc Natl Acad Sci USA. 1996; 93(10):4604–4607. [PubMed: 8643450]

Biggar SR, Crabtree GR. Chemically regulated transcription factors reveal the persistence of repressor-resistant transcription after disrupting activator function. J Biol Chem. 2000; 275(33):25381. [PubMed: 10801867]

Biggar SR, Crabtree GR. Cell signaling can direct either binary or graded transcriptional responses. EMBO J. 2001; 20(12):3167. [PubMed: 11406593]

Blakley RL. Crystalline Dihydropteroylglutamic Acid. Nature. 1960; 188:231–232.

Bogan AA, Thorn KS. Anatomy of hot spots in protein interfaces. J Mol Biol. 1998; 280:1–9. [PubMed: 9653027]

Brooijmans N, Sharp KA, et al. Stability of macromolecular complexes. Proteins: Structure, Function, and Genetics. 2002; 48:645–653.

Camacho CJ, Ma H, et al. Scoring a diverse set of high-quality docked conformations: A metascore based on electrostatic and desolvation interactions. Proteins-Structure Function and Bioinformatics. 2006; 63(4):868–877.

Carlotti F, Zaldumbide A, et al. Development of an inducible suicide gene system based on human caspase 8. Cancer Gene Ther. 2005; 12:627–639. [PubMed: 15746943]

Carlson JCT, Jena SS, et al. Chemically Controlled Self-Assembly of Protein Nanorings. J Am Chem Soc. 2006; 128:7630. [PubMed: 16756320]

Carlson JCT, Kanter A, et al. Designing Protein Dimerizers: The Importance of Ligand Conformational Equilibria. J Am Chem Soc. 2003; 125:1501. [PubMed: 12568609]

Carlson JCT, Kanter A, et al. Designing protein dimerizers: The importance of ligand conformational equilibria. J Amer Chem Soc. 2003; 125:1501–1507. [PubMed: 12568609]

Carugo OF. Prediction of polypeptide fragments exposed to the solvent. In Silico Biol. 2003; 3(4):417–428. [PubMed: 12954085]

Cheng J, Yu L, et al. Dimerization through the Catalytic Domain Is Essential for MEKK2 Activation. J Biol Chem. 2005; 280(14):13477. [PubMed: 15695508]

Choi J, Chen J, et al. Structure of the FKBP12-rapamycin complex interacting with the binding domain of human FRAP. Science. 1996; 273(5272):239–242. [PubMed: 8662507]

Chou TF, So C, et al. Enzyme Nanorings. Nano Lett. 2008; 2(12):2519.

Chowdhury SM, Shi L, et al. A Method for Investigating Protein-Protein Interactions Related to Salmonella Typhimurium Pathogenesis. Journal of Proteome Research. 2009; 8(3):1504–1514. [PubMed: 19206470]

Clackson T, Wells JA. A Hot Spot of Binding Energy in a Hormone-Receptor Interface. Science. 1995; 267(5196):383–386. [PubMed: 7529940]

Cochran AG. Antagonists of protein-protein interactions. Chem Biol. 2000; 7(4):R85–R94. [PubMed: 10779412]

Crowley PB, Otting G, et al. Hydrophobic interactions in a cyanobacterial plastocyanin-cytochrome f complex. J Am Chem Soc. 2001; 123(43):10444–10453. [PubMed: 11673974]

Cukuroglu E, Gursoy A, et al. HotRegion: a database of predicted hot spot clusters. Nucleic Acids Research. 2012; 40(D1):D829–D833. [PubMed: 22080558]

Cunningham BC, Wells JA. Rational design of receptor specific variants of human growth hormone. Proc Natl Acad Sci USA. 1991; 88(8):3407–3411. [PubMed: 2014261]

Dotan N, Arad D, et al. Self-assembly of a tetrahedral lectin into predesigned, diamond-like protein crystals. Angew Chem Int Ed. 1999; 38(16):2363–2366.

Elcock AH, McCammon JA. Identification of Protein Oligomerisation States by Analysis of Interface Conservation. Proc Natl Acad Sci USA. 2001; 98:2990–2994. [PubMed: 11248019]

Farrar M, Alberola-Ila J, et al. Activation of the Raf-1 kinase cascade by coumermycin-induced dimerization. Nature. 1996; 383:178–181. [PubMed: 8774884]

Fegan A, White BR, et al. Chemically Controlled Protein Assembly: Techniques and Applications. Chem Rev. 2010; 110(6):3315–3336. [PubMed: 20353181]

Garner AL, Janda KD. Protein-Protein Interactions and Cancer: Targeting the Central Dogma. Current Topics in Medicinal Chemistry. 2011; 11(3):258–280. [PubMed: 21320057]

George N, Pick H, et al. Specific labeling of cell surface proteins with chemically diverse compounds. J Am Chem Soc. 2004; 126(29):8896. [PubMed: 15264811]

Geppert T, Hoy B, et al. Context-Based Identification of Protein-Protein Interfaces and “Hot-Spot Residues”. Chemistry & Biology. 2011; 18(3):344–353. [PubMed: 21439479]

Gestwicki JE, Crabtree GR, et al. Harnessing chaperones to generate small-molecule inhibitors of amyloid beta aggregation. Science. 2004; 306(5697):865. [PubMed: 15514157]

Glaser F, Steinberg DM, et al. Residue frequencies and pairing preferences at protein–protein interfaces. Proteins: Structure, Function, and Bioinformatics. 2001; 43(2):89–102.

Gohlke H, Case DA. Converging free energy estimates: Mm-pb(gb)sa studies on the protein-protein complex ras-raf. J Comp Chem. 2004; 25:238–250. [PubMed: 14648622]

Hall DH, Grove LE, et al. Robust Identification of Binding Hot Spots Using Continuum Electrostatics: Application to Hen Egg-White Lysozyme. Journal of the American Chemical Society. 2011; 133(51):20668–20671. [PubMed: 22092261]

Hendsch ZS, Jonsson T, et al. Protein stabilization by removal of unsatisfied polar groups: Computational approaches and experimental tests. Biochemistry. 1996; 35:7621–7625. [PubMed: 8672461]

Hendsch ZS, Nohaile MJ, et al. Preferential heterodimer formation via undercompenstated electrostatic interactions. J Am Chem Soc. 2001; 123:1264–1265. [PubMed: 11456695]

Hendsch ZS, Tidor B. Electrostatic interactions in the GCN4 leucine zipper: substantial contributions arise from intramolecular interactions enhanced on binding. Protein Sci. 1999; 8(7):1381–1392. [PubMed: 10422826]

Johnson LM, Horne WS, et al. Broad Distribution of Energetically Important Contacts across an Extended Protein Interface. Journal of the American Chemical Society. 2011; 133(26):10038–10041. [PubMed: 21644542]

Jones S, Thornton JM. Principles of protein-protein interactions. Proc Natl Acad Sci USA. 1996; 93(1):13–20. [PubMed: 8552589]

Karanicolas J, Com JE, et al. A De Novo Protein Binding Pair By Computational Design and Directed Evolution. Molecular Cell. 2011; 42(2):250–260. [PubMed: 21458342]

Keppler A, Kindermann M, et al. Labeling of fusion proteins of O6-alkylguanine-DNA alkyltransferase with small molecules in vivo and in vitro. Methods. 2004; 32(4):437. [PubMed: 15003606]

Keskin O, Gursoy A, et al. Principles of protein-protein interactions: what are the preferred ways for proteins to interact? Chem Rev. 2008; 108(4):1225–1244. [PubMed: 18355092]

Kitov PI, Lipinski T, et al. An entropically efficient supramolecular inhibition strategy for Shiga toxins. Angew Chem Int Ed. 2008; 47(4):672–676.

Kley N. Chemical dimerizers and three-hybrid systems: scanning the proteome for targets of organic small molecules. Chem Biol. 2004; 11(5):599–608. [PubMed: 15157871]

Kobe B, Kajava AV. The leucine-rich repeat (lrr) as a protein recognition motif. Curr Opin Struct Biol. 2001; 11:725–732. [PubMed: 11751054]

Kopytek SJ, Standaert RF, et al. Chemically induced dimerization of dihydrofolate reductase by a homobifunctional dimer of methotrexate. Chem Biol. 2000; 7(5):313. [PubMed: 10801470]

Lemercier G, Gendreizig S, et al. Inducing and Sensing Protein-Protein Interactions in Living Cells by Selective Cross-linking. Angew Chem Int Ed. 2007; 46(23):4281.

Lewis SM, Kuhlman BA. Anchored Design of Protein-Protein Interfaces. Plos One. 2011; 6(6)

Li Q, Hapka D, et al. Self-Assembly of Antibodies by Chemical Induction. Angewandte Chemie-International Edition. 2008; 47(52):10179–10182. [PubMed: 19025747]

Li Q, So CR, et al. Chemically Self-Assembled Antibody Nanorings (CSANs): Design and Characterization of an Anti-CD3 IgM Biomimetic. J Amer Chem Soc. 2010; 132(48):17247–17257. [PubMed: 21077608]

Liberles SD, Diver ST, et al. Inducible gene expression and protein translocation using nontoxic ligands identified by a mammalian three-hybrid screen. Proc Natl Acad Sci USA. 1997; 94:7825–7830. [PubMed: 9223271]

Licitra EJ, Liu JO. A three-hybrid system for detecting small ligand-protein receptor interactions. Proc Natl Acad Sci USA. 1996; 93(23):12817. [PubMed: 8917502]

Liu JY, Li ZM, et al. Critical Residue That Promotes Protein Dimerization: A Story of Partially Exposed Phe(25) in 14-3-3 sigma. Journal of Chemical Information and Modeling. 2011; 51(10):2612–2625. [PubMed: 21870863]

Lo Conte L, Chothia C, et al. The atomic structure of protein-protein recognition sites. J Mol Biol. 1999; 285(5):2177–2198. [PubMed: 9925793]

Lowman HB, Cunningham BC, et al. Mutational analysis and protein engineering of receptor-binding determinants in human placental lactogen. J Biol Chem. 1991; 266(17):10982–10988. [PubMed: 2040614]

Luo Z, Tzivion G, et al. Oligomerization activates c-raf-1 through a ras-dependent mechanism. Nature. 1996; 383(181–5)

Mandell DJ, Kortemme T. Computer-aided design of functional protein interactions. Nature Chemical Biology. 2009; 5(11):797–807. [PubMed: 19841629]

Marcotte EM, Pellegrini M, et al. Detecting protein function and protein-protein interactions from genome sequences. Science. 1999; 285(5428):751–753. [PubMed: 10427000]

Massova I, Kollman PA. Computational Alanine Scanning To Probe Protein–Protein Interactions: A Novel Approach To Evaluate Binding Free Energies. J Am Chem Soc. 1999; 121(36):8133–8143.

Meireles LMC, Mustata G. Discovery of Modulators of Protein-Protein Interactions: Current Approaches and Limitations. Current Topics in Medicinal Chemistry. 2011; 11(3):248–257. [PubMed: 21320056]

Mootz HD, Blum ES, et al. Conditional Protein Splicing: A New Tool to Control Protein Structure and Function in Vitro and in Vivo. J Am Chem Soc. 2003; 125(35):10561. [PubMed: 12940738]

Mootz HD, Muir TW. Protein Splicing Triggered by a Small Molecule. J Am Chem Soc. 2002; 124:9044. [PubMed: 12148996]

Morell M, Espargaro A, et al. Detection of transient protein–protein interactions by bimolecular fluorescence complementation: The Abl-SH3 case. Proteomics. 2007; 7(7):1023–1036. [PubMed: 17352427]

Nakamura T, Iwakura M. Circular permutation analysis as a method for distinction of functional elements in the m20 loop of escherichia coli dihydrofolate reductase. J Biol Chem. 1999; 274:19041–19047. [PubMed: 10383405]

Neff T, Blau CA. Pharmacologically regulated cell therapy. Blood. 2001; 97(9):2535. [PubMed: 11313238]

Nyanguile O, Uesugi M, et al. A nonnatural transcriptional coactivator. Proc Natl Acad Sci USA. 1997; 94:13402. [PubMed: 9391036]

O'Shea EK, Rutkowski R, et al. Mechanism of specificity in the Fos-Jun oncoprotein heterodimer. Cell. 1992; 68(4):699–708. [PubMed: 1739975]

O'Shea EK, Rutkowski R, et al. Preferential heterodimer formation by isolated leucine zippers from fos and jun. Science. 1989; 245:646–648. [PubMed: 2503872]

Ofran Y, Rost B. Analysing six types of protein-protein interfaces. J Mol Biol. 2003; 325(2):377–387. [PubMed: 12488102]

Padilla JE, Colovos C, et al. Nanohedra: using symmetry to design self assembling protein cages, layers, crystals, and filaments. Proc Natl Acad Sci USA. 2001; 98(5):2217. [PubMed: 11226219]

Reichmann D, Rahat O, et al. The molecular architecture of protein-protein binding sites. Curr Opin Struct Biol. 2007; 17:67–76. [PubMed: 17239579]

Reilly MT, Cunningham KA, et al. Protein-protein interactions as therapeutic targets in neuropsychopharmacology. Neuropsychopharmacology. 2009; 34(1):247–248.

Rele S, Song Y, et al. D-periodic collagen-mimetic microfibers. J Am Chem Soc. 2007; 129(47): 14780–14787. [PubMed: 17985903]

Ringler P, Schulz GE. Self-assembly of proteins into designed networks. Science. 2003; 302(5642): 106. [PubMed: 14526081]

Rosowsky A, Forsch RA, et al. Methotrexate analogs. 22. Synthesis, dihydrofolate reductase affinity, cytotoxicity, and in vivo antitumor activity of some putative degradation products of methotrexate-poly(L-lysine) conjugates. J Med Chem. 1984; 27(7):888–893. [PubMed: 6737432]

Rowe SP, Casey RJ, et al. Transcriptional Up-regulation in Cells Mediated by a Small Molecule. J Am Chem Soc. 2007; 129:10654. [PubMed: 17691790]

Salwinski L, Miller CS, et al. The database of interacting proteins: 2004 update. Nucleic Acids Res. 2004; 32:D449–451. [PubMed: 14681454]

Sawaya MR, Kraut J. Loop and domain movements in the mechanism of e. Coli dihydrofolate reductase: Crystallographic evidence. Biochemistry. 1997; 36:586–603. [PubMed: 9012674]

Schwartz EC, Saez L, et al. Post-translational enzyme activation in an animal via optimized conditional protein splicing. Nat Chem Biol. 2007; 3(1):50. [PubMed: 17128262]

Seeger DR, Cosulich DB, et al. Analogs of Pteroylglutamic Acid. III. 4-Amino Derivatives. J Am Chem Soc. 1949; 71:1753–1758.

Sheinerman FB, Norel R, et al. On the role of electrostatic interactions in the design of protein-protein interfaces. J Mol Biol. 2002; 318(1):161–177. [PubMed: 12054776]

Sillerud LO, Larson RS. Design and structure of peptide and peptidomimetic antagonists of protein-protein interaction. Curr Protein Pept Sci. 2005; 6(2):151–169. [PubMed: 15853652]

Smith CA, Kortemme T. Predicting the Tolerated Sequences for Proteins and Protein Interfaces Using RosettaBackrub Flexible Backbone Design. Plos One. 2011; 6(7)

Smith GP. Filamentous fusion phage: Novel expression vectors that display cloned antigens on the virion surface. Science. 1985; 228:1315–1317. [PubMed: 4001944]

Spencer DM, Wandless TJ, et al. Controlling signal transduction with synthetic ligands. Science. 1993; 262:1019. [PubMed: 7694365]

Stankunas K, Crabtree GR. Exploiting protein destruction for constructive use. Proc Natl Acad Sci USA. 2007; 104(28):11511. [PubMed: 17606901]

Taira K, Benkovic SJ. Evaluation of the importance of hydrophobic interactions in drug binding to dihydrofolate reductase. J Med Chem. 1988; 31(1):129–137. [PubMed: 3275776]

Tang C, Iwahara J, et al. Visualization of transient encounter complexes in protein-protein association. Nature. 2006; 444:383–386. [PubMed: 17051159]

Thorn KS, Bogan AA. Asedb: A database of alanine mutations and their effects on the free energy of binding in protein interactions. Bioinformatics. 2001; 17:284–285. [PubMed: 11294795]

Tsai CJ, Lin SL, et al. Studies of protein-protein interfaces: a statistical analysis of the hydrophobic effect. Protein Sci. 1997; 6(1):53–64. [PubMed: 9007976]

Tsai CJ, Taylor R, et al. The packing density in proteins: Standard radii and volumes. J Mol Biol. 1999; 290:253–266. [PubMed: 10388571]

Uetz P, Goit L, et al. A comprehensive analysis of proteinprotein interactions in Saccharomyces cerevisiae. Nature. 1999; 403(6770):623–627.

Vaskar IA, Aflalo C. Hydrophobic docking: A proposed enhancement to molecular recognition techniques. Proteins. 1994; 20:320–329. [PubMed: 7731951]

Walls PH, Sternberg MJE. New algorithm to model protein-protein recognition based on surface complementarity – Applications to antibody-antigen docking. J Mol Biol. 1992; 228:277–297. [PubMed: 1280302]

Whitney ML, Otto KG, et al. Control of myoblast proliferation with a synthetic ligand. J Biol Chem. 2001; 276(44):41191. [PubMed: 11502737]

Xu MQ, Evans TCJ. Recent advances in protein splicing: manipulating proteins in vitro and in vivo. Curr Opin Biotechnol. 2005; 16:440. [PubMed: 16026977]

Young L, Jernigan RL, et al. A role for surface hydrophobicity in protein-protein recognition. Protein Sci. 1994; 3(5):717–729. [PubMed: 8061602]

Zhao Z, Zhao M, et al. Gene transfer of the Runx2 transcription factor enhances osteogenic activity of bone marrow stromal cells in vitro and in viv. Mol Ther. 2005; 12(2):247–253. [PubMed: 16043096]

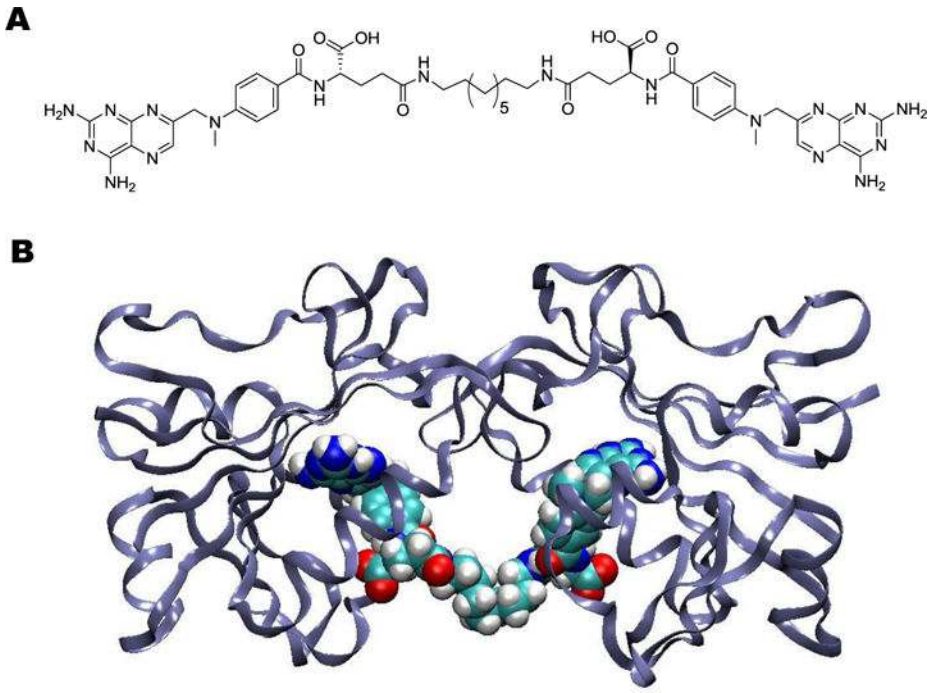

Figure 1.
Structures of a) bis-MTX-C9 (MTX_2C9) and b) the chemically induced DHFR dimer.

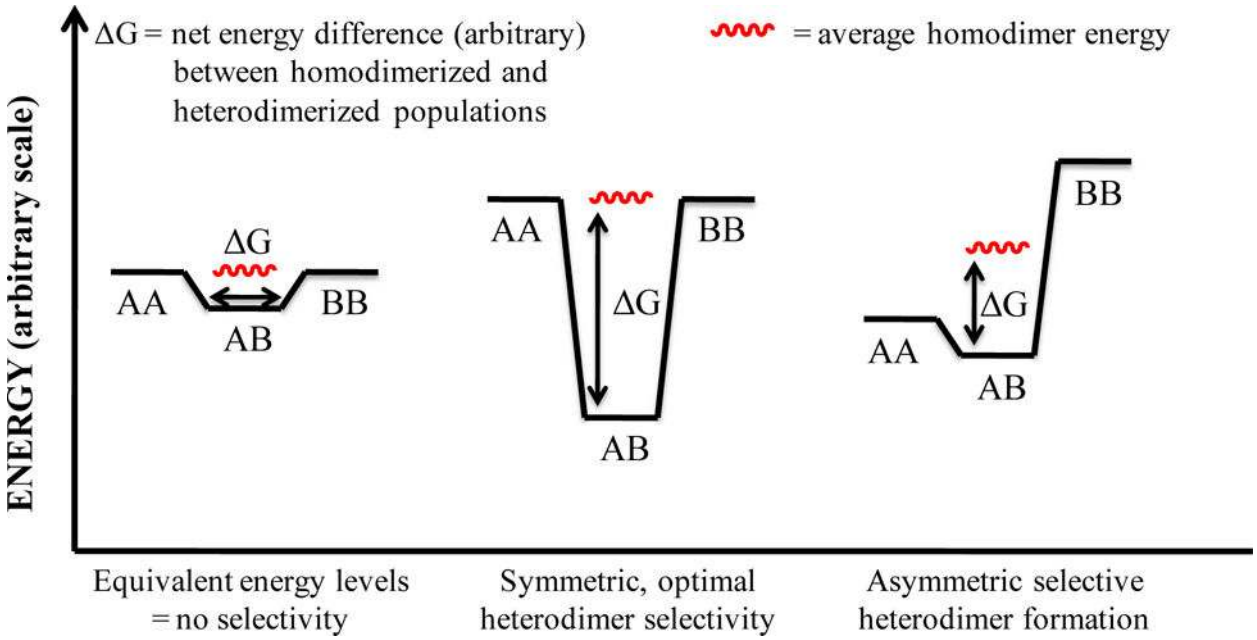

Figure 2.
Dimerization energy landscape – the energetics of heterodimer selectivity.

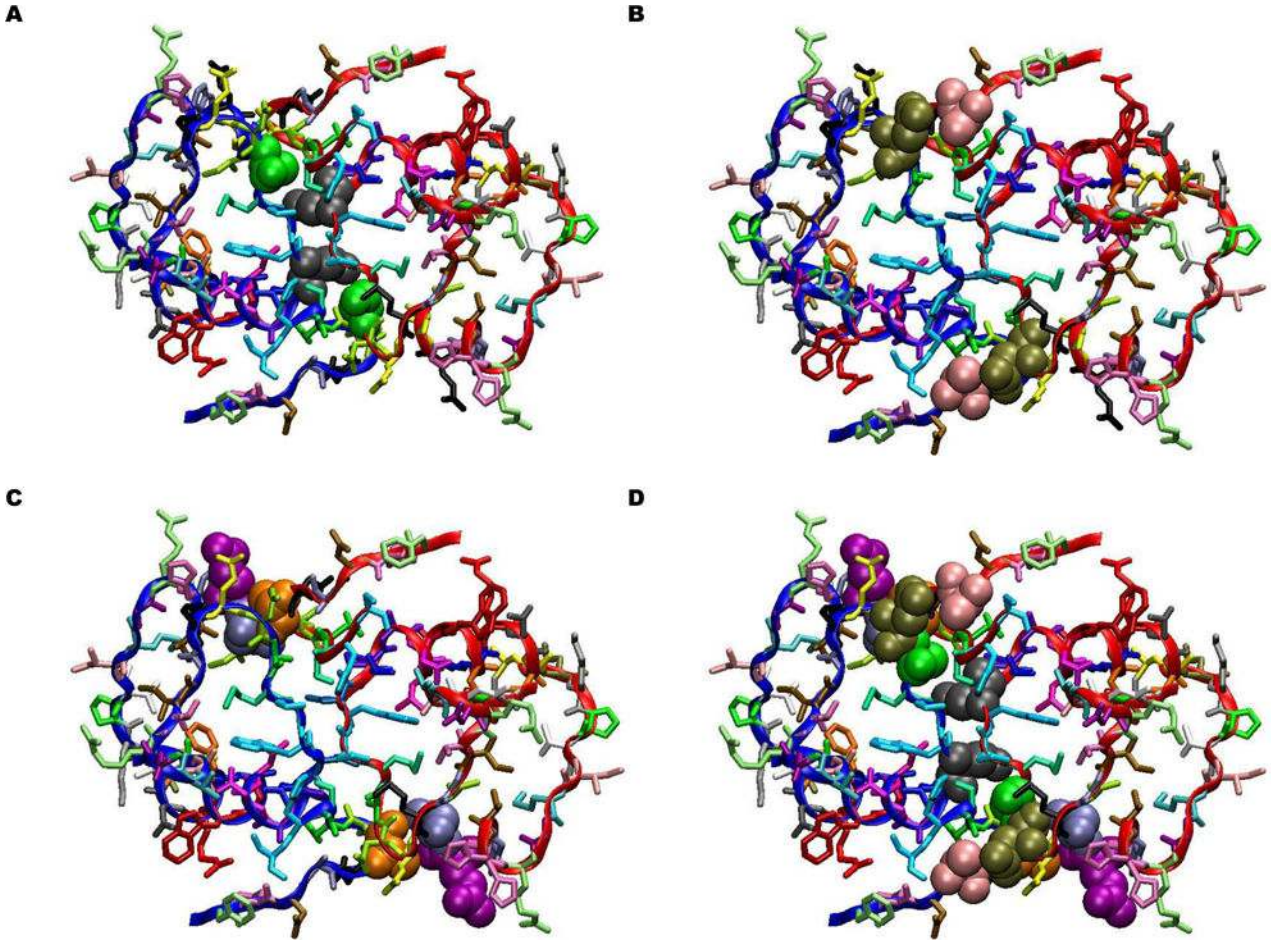

Figure 3.

Views of key contacts at the ecDHFR dimer interface. The truncated protein shown represents the interfacial portion of the dimer, with residues of interest rendered as VDW. Different DHFR monomers are represented by the blue and red ribbons. The entire structure is rotated 90° about the longitudinal axis as seen in Figure 1. A) Ala19 (green) and Asn23 (gray). B) Asn18 (tan) and Ala143 (pink). C) Glu48 (purple), Ser49 (blue), and Ala145 (orange). D) All residues in a–c.

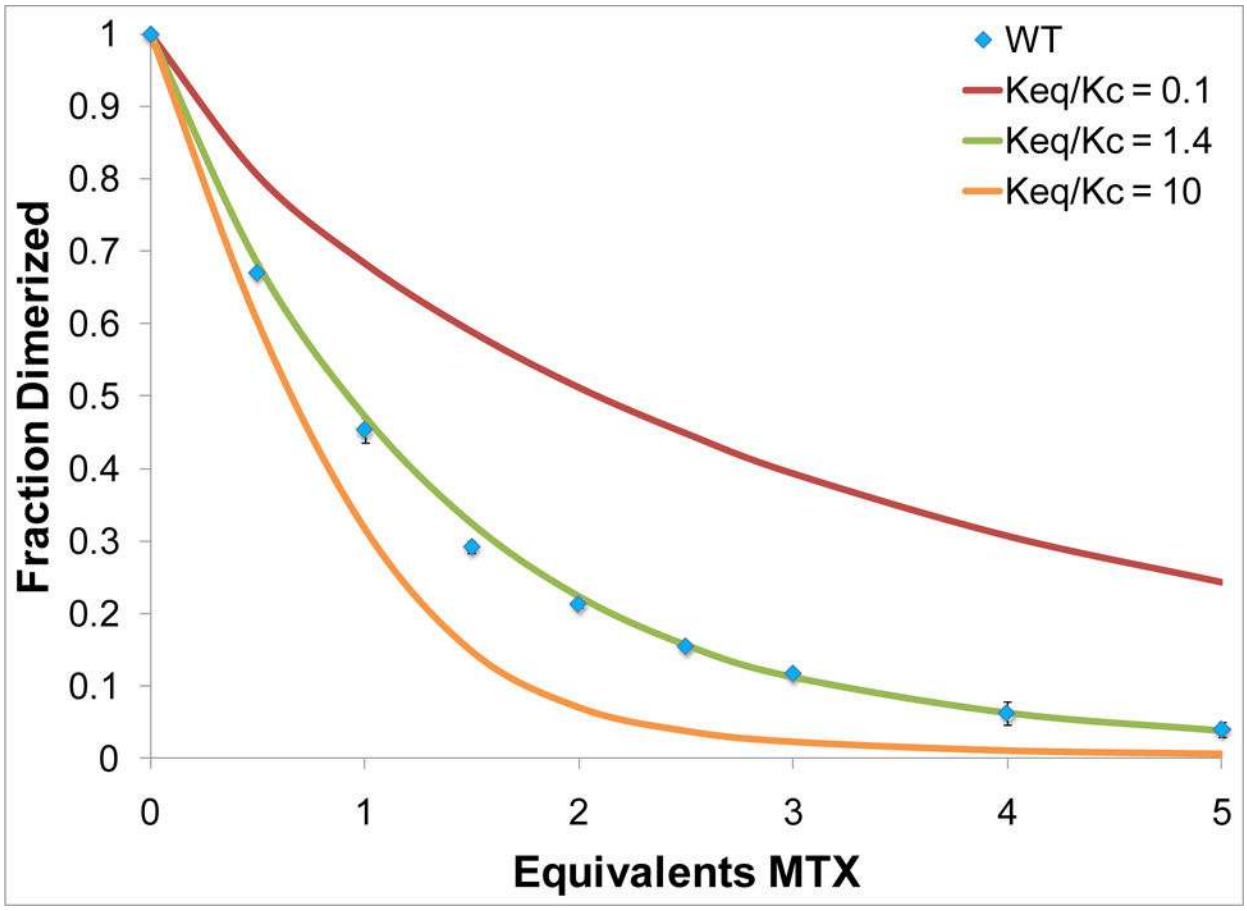

Figure 4.

Typical competition denaturation curve highlighting K_{eq}/K_c ratios of 0.1, 1.4, and 10. Data points for wild-type denaturation represent the effect of adding 0.5 to 5.0 equivalents of MTX to a MTX_2C9-induced dimer. Error bars are derived from the standard deviation in three independent experiments. Fit lines display the effects of varying the K_{eq}/K_c ratio in Equation 1.

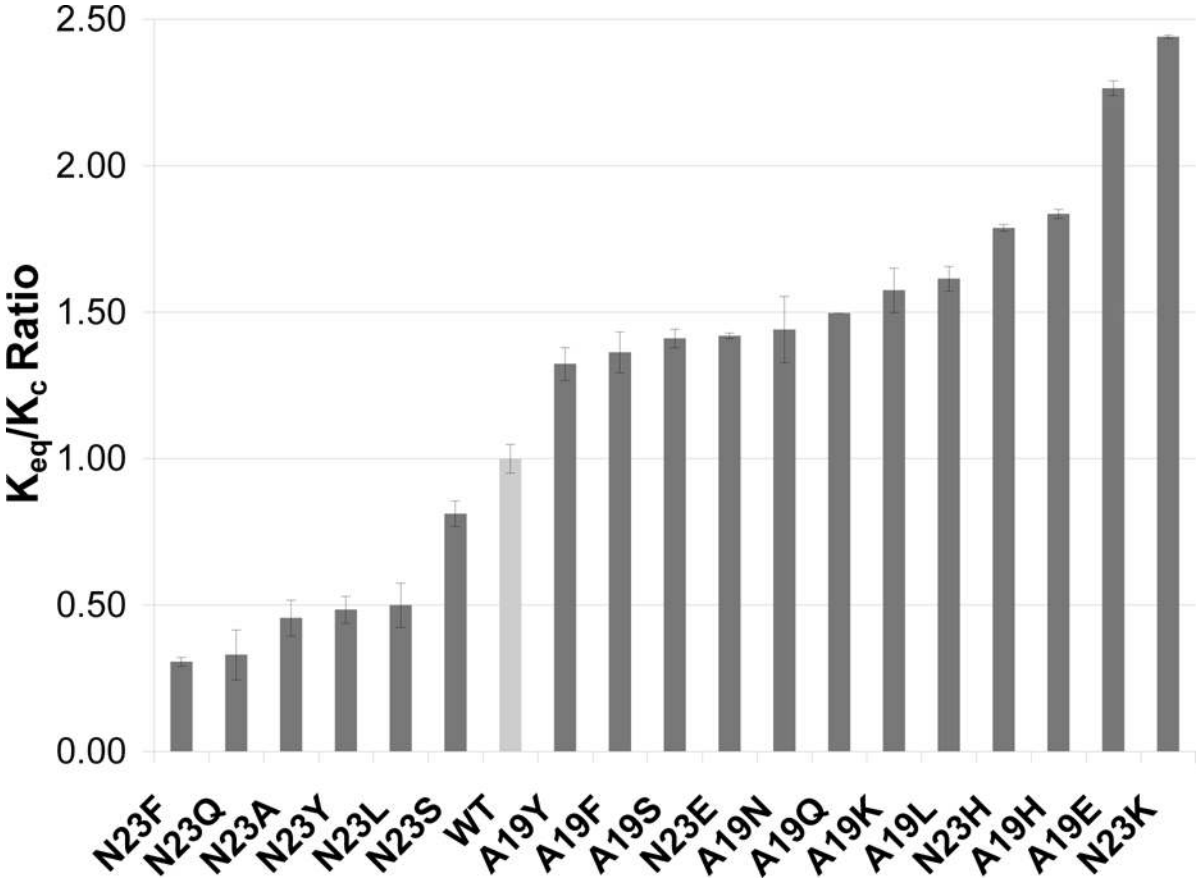

Figure 5.

Results of competition assays for each DHFR variant studied. Error bars represent the range of ratios determined from error analysis.

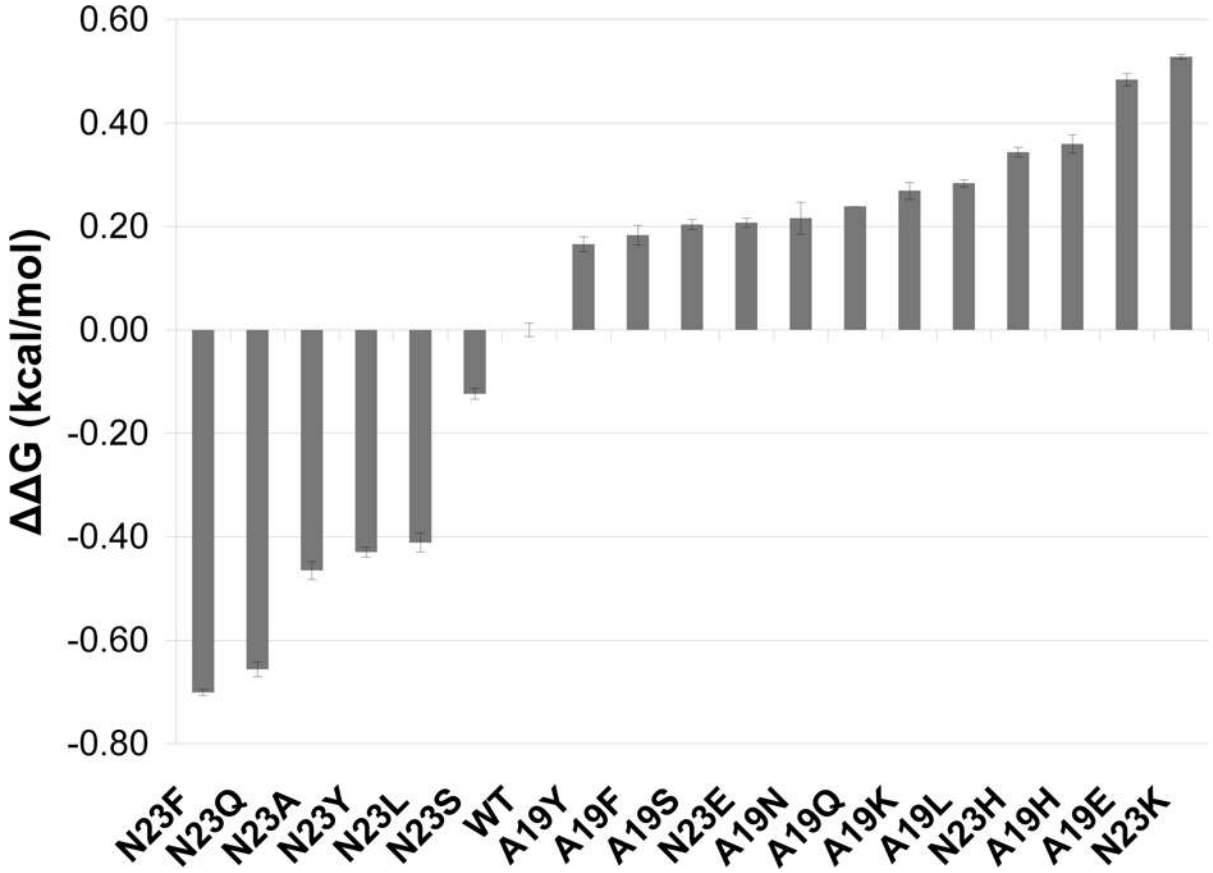

Figure 6.
Energetic contribution to dimer stability from interfacial mutations.

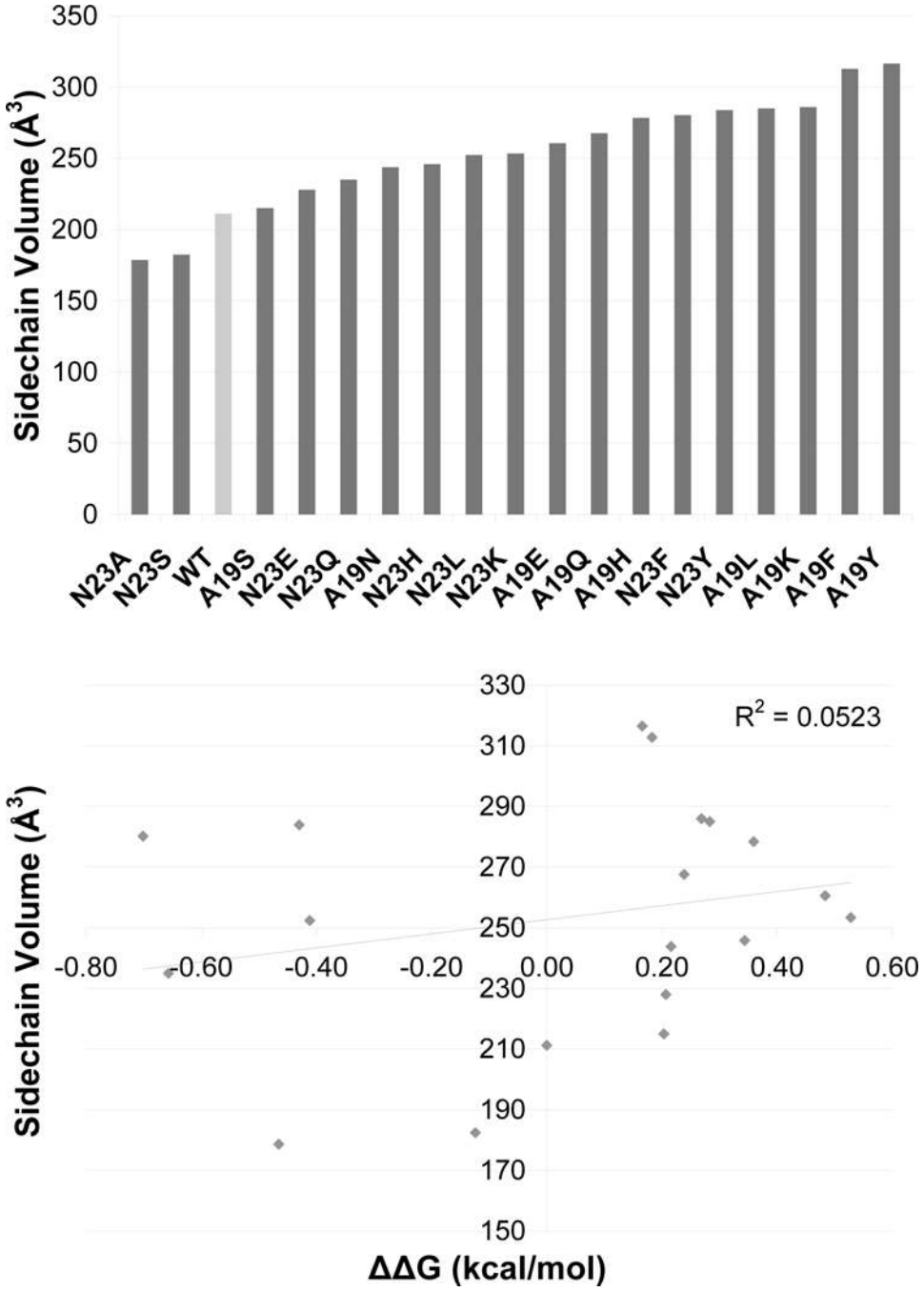

Figure 7.
Total residue 19/23 sidechain volumes (top panel) and their relationship to ΔΔG (bottom panel).

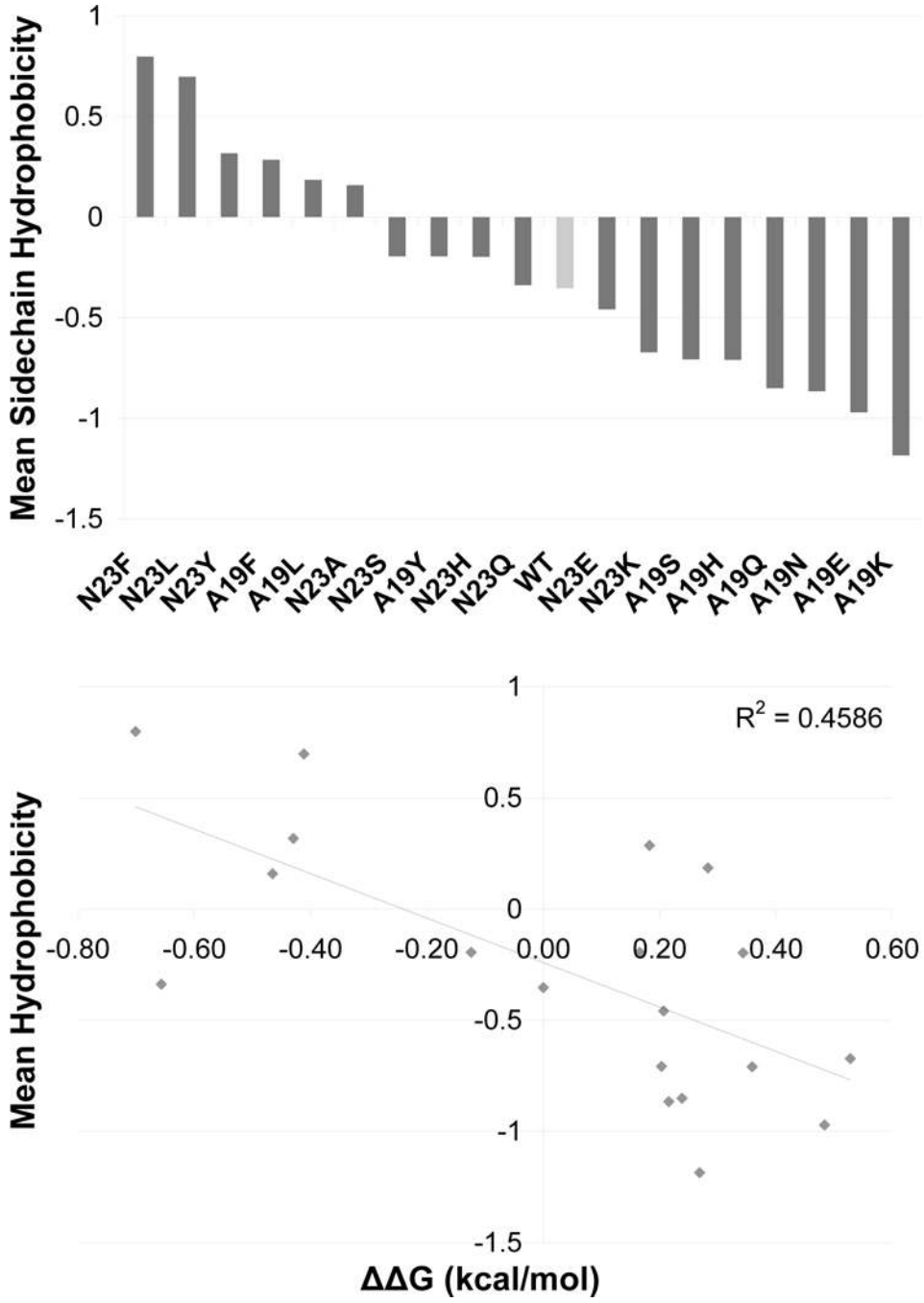

Figure 8.

Residue 19/23 mean hydrophobicity (top panel) and negative (stabilizing) relationship to ΔΔG (bottom panel).

Table 1

Sites of interfacial contacts in the DHFR dimer interface. Residue pairs are classified by the type of contact: sidechain-sidechain (S-S), sidechain-backbone (S-B), and backbone-backbone (B-B).

Residue A	Residue B	Type of Contact
Asn18	Ala143	S-S
	Asp144	S-B
Ala19	Asn23	S-S
Ala19	Asp144	B-B
Asn23	Asn23	S-S
Ala145	Glu48	S-S
	Ser49	
Gln146	Gly51	S-S
	Glu48	
	Ser49	
Ser148	Pro21	S-B, S-S

Table 2

WT and Mutant K_d data.

Protein	K_d (pM)	Protein	K_d (pM)
WT	695 ± 253	A19Y	402 ± 106
N23Y	894 ± 267	A19S	606 ± 283
N23S	462 ± 269	A19Q	462 ± 166
N23Q	766 ± 326	A19L	583 ± 377
N23L	1141 ± 311	A19H	319 ± 176
N23F	2972 ± 966	A19F	327 ± 136

Table 3

Ratios of mutant:WT K_{eq}/K_c values and associated ΔΔG values.

Protein	Mutant/WT K_{eq}/K_c Ratio	ΔΔG (kcal/mol)	Protein	Mutant/WT K_{eq}/K_c Ratio	ΔΔG (kcal/mol)
A19E	2.26	0.48 ± 0.01	N23A	0.46	−0.47 ± 0.01
A19F	1.36	0.18 ± 0.02	N23E	1.42	0.21 ± 0.03
A19H	1.84	0.36 ± 0.01	N23F	0.31	−0.70 ± 0.00
A19K	1.57	0.27 ± 0.02	N23H	1.79	0.34 ± 0.02
A19L	1.61	0.28 ± 0.01	N23K	2.44	0.53 ± 0.01
A19N	1.44	0.22 ± 0.01	N23L	0.50	−0.41 ± 0.01
A19Q	1.50	0.24 ± 0.01	N23Q	0.33	−0.66 ± 0.02
A19S	1.41	0.20 ± 0.02	N23S	0.81	−0.12 ± 0.01
A19Y	1.32	0.17 ± 0.01	N23Y	0.48	−0.43 ± 0.00